01 Dec 1982

Angular Scattering In Slow Multiple-charged Ion, Atom Collisions

Ronald E. Olson
Missouri University of Science and Technology, olson@mst.edu

M. Kimura

Recommended Citation

R. E. Olson and M. Kimura, "Angular Scattering In Slow Multiple-charged Ion, Atom Collisions," *Journal of Physics B: Atomic and Molecular Physics*, vol. 15, no. 22, pp. 4231 - 4238, article no. 022, IOP Publishing, Dec 1982.
The definitive version is available at https://doi.org/10.1088/0022-3700/15/22/022

Angular scattering in slow multiple-charged ion, atom collisions

J. Phys. B: At. Mol. Phys. **15** (1982) 4231–4238. Printed in Great Britain

Angular scattering in slow multiply-charged ion, atom collisions

R E Olson and M Kimura

Physics Department, University of Missouri-Rolla, Rolla, MO 65401 USA

Received 28 June 1982

Abstract. The $C^{6+}+H$ system is used to illustrate the importance of large-angle scattering in collisions between slow multiply-charged ions and atoms. A quantum mechanical description based on a diabatic formalism of the collision system is used to obtain differential cross sections for electron capture in the relative velocity range $v = 1\times10^7$ to 3×10^7 cm s^{-1} ($E_{cm}\simeq 48$ to 430 eV). The threshold for angular scattering is at $E\theta \simeq$ 0.2 keV deg which correlates with the curve crossing between initial and final molecular states located at $R_x \simeq 8a_0$. The centre-of-mass acceptance angles required to observe fixed fractions of the total electron capture cross sections are presented. Representative examples for the detection of 90% of the total electron capture cross section requires angular acceptances of 78° at 1×10^7 cm s^{-1} and 8.5° at 3×10^7 cm s^{-1}.

1. Introduction

Advances in experimental techniques have made possible the measurement of electron capture cross sections for low-energy collisions of multiply-charged atoms with atomic targets. The development of a laser ion source by Phaneuf (1981) has led to the measurement of $C^{q+}+H$ cross sections in the range of 11 to 387 eV amu^{-1}. Recoil ions produced by the passage of a high-energy, highly charged ion beam through a gas cell have made possible cross section measurements down to 100 eV/projectile charge in $Ar^{q+}+Ne$ systems (Justiniano *et al* 1981) and product state determinations in $Ne^{q+}+Ne$ systems (Beyer *et al* 1980).

However, a serious consideration for cross section measurements at low energies is the angular scattering of the products. For the general reaction

$$A^{q+}+B\rightarrow A^{(q-1)+}+B^{+} \tag{1}$$

the incident channel is covalent and imparts little deflection to the particles at moderately large impact parameters. In contrast, after electron capture, the ionic products are deflected by a strong Coulomb repulsive potential of the form $+(q-1)e^2/R$, where R is the internuclear separation. In general, reaction (1) is exothermic and induced by curve crossing interactions in the range $R\simeq 5$ to $10\,a_0$ for incident charge states $q\simeq 4$ to 10 (Olson and Salop 1976). Thus, the deflection is appreciable and must be considered in the design of experimental set-ups. Hasted and colleagues (Makhdis *et al* 1976, Sharma *et al* 1979) recognised the importance of the angular scattering very early and employed the relationship between deflection angle and impact parameter to perform collision spectroscopy measurements for many systems of the reaction (1) prototype.

0022-3700/82/224231+08$02.00

It is the purpose of this paper to emphasise the importance of the angular scattering in low-energy measurements. As an illustrative example we have chosen the $C^{6+}+H$ system

$$C^{6+}+H \rightarrow C^{5+}+H^{+} \tag{2}$$

because the dominant curve crossing interaction lies at $R \simeq 8\,a_0$ and the system has been fully tested (Green *et al* 1981). A two-state calculation is also valid to determine the total cross section at low energies with an accuracy of approximately $\pm 25\%$. Thus, in this paper we are able to present a representative example of the differential cross sections and the acceptance angles required to observe fixed percentages of the total cross section for relative velocities from 1×10^7 to 3×10^7 cm s^{-1}.

2. Theory

Since we are concerned with the low-velocity differential scattering for reaction (2), it is necessary to use a quantum mechanical treatment to achieve a valid result. In the present study, we employed two states, $5g\sigma$ (incident channel diabatically connected to $C^{6+}+H$) and $4f\sigma$ ($C^{5+}(n=4)+H^{+}$) which are connected by strong radial coupling at an avoided crossing at $R \simeq 8\,a_0$. These adiabatic states and their $\partial/\partial R$ coupling term were transformed into the diabatic representation where the radial coupling matrix element vanishes and the off-diagonal elements of the potential coupling matrix induce the transitions between the levels.

The scattering problem then requires the numerical solution of the coupled equations (Smith 1969):

$$\left(-\frac{1}{2\mu}\nabla_R^2\mathbf{I}-\mathbf{V}(R)+E\mathbf{I}\right)\boldsymbol{F}(R)=\mathbf{0} \tag{3}$$

where $\mathbf{V}(R)$ is the potential matrix

$$\mathbf{V}(R)=\mathbf{W}^{-1}(R)\boldsymbol{\varepsilon}(R)\mathbf{W}(R) \tag{4}$$

and $\boldsymbol{\varepsilon}(R)$ are the eigenenergies of the electronic Hamiltonian obtained using the Born–Oppenheimer (BO) approximation. The transformation matrix for the two-state case is given by

$$\mathbf{W}(R)=\begin{pmatrix}\cos\theta(R) & \sin\theta(R)\\ -\sin\theta(R) & \cos\theta(R)\end{pmatrix} \tag{5}$$

where

$$\theta(R)=\int_R^{\infty} P_{12}(R')\,\mathrm{d}R' \tag{6}$$

with $P_{12}(R)$ being the radial coupling matrix elements determined in the adiabatic frame:

$$P_{12}(R)=\left\langle \phi_2^{\mathrm{BO}}(\boldsymbol{r},R)\left|-\mathrm{i}\hbar\frac{\partial}{\partial R}\right|\phi_1^{\mathrm{BO}}(\boldsymbol{r},R)\right\rangle. \tag{7}$$

The radial wavefunctions $\boldsymbol{F}(R)$ have the asymptotic form

$$F_{if}(R)\underset{R\rightarrow\infty}{\sim}\delta_{if}U_i^l(k_i,R)-S_{if}^l U_f^l(k_f,R) \tag{8}$$

where S^l_{if} is the scattering S matrix for a given orbital angular momentum quantum number l. For the elastic channel i, U^l_i are composed of regular and irregular Riccati–Bessel functions (Calogero 1967)

$$U^l_i = n_l \pm i j_l. \tag{9}$$

For the inelastic channel f, U^l_f can be written as a linear combination of regular and irregular Coulomb wavefunctions (Messiah 1958)

$$U^l_f = \exp(\mp i\delta_l)(G_l(k_f R, \eta) \pm iF_l(k_f R, \eta)) \tag{10}$$

where δ_l is the Coulomb phaseshift

$$\delta_l = \arg \Gamma(l+1+i\eta) \tag{11}$$

and

$$\eta = (q-1)e^2/\hbar v. \tag{12}$$

To solve equation (3) numerically, we have employed the logarithmic derivative method of Johnson (1973) with asymptotic matching conditions using equation (9) for the elastic channel and equation (10) for the inelastic channel. The radial coupling matrix elements in the adiabatic representation, equation (7), have been calculated with electron translational factor corrections (Thorson *et al* 1981). These matrix elements were fitted to a Lorentzian form (Melius and Goddard 1974) and used in the evaluation of $\theta(R)$, equation (6). The deviation from this Lorentzian form was less than $\pm 15\%$ for $R \geq 5\ a_0$. The diabatic interaction and coupling potentials used in our study are presented in figure 1. Cross section determinations were made using standard procedures.

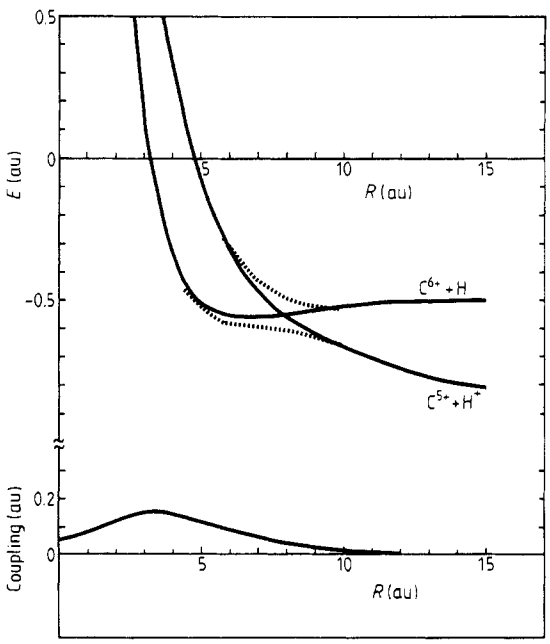

Figure 1. The full curves show the diabatic potentials and coupling matrix elements used for the $C^{6+} + H$ calculations. The dotted curves denote the adiabatic potential around the avoided crossing at $R_x \simeq 8\ a_0$.

3. Results and discussion

As an example of the computed transition probabilities for reaction (2), we show the results for $v = 1 \times 10^7$ cm s^{-1} in figure 2. Transitions occur for impact parameters $b \leqslant 8.5\, a_0$ and display characteristic oscillatory structure due to a curve crossing interaction with two possible trajectories for internuclear separations less than R_x.

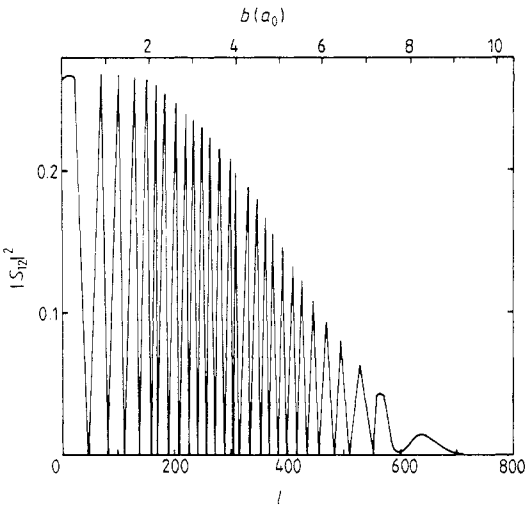

Figure 2. Calculated electron capture transition probabilities for $C^{6+}+H$ at $v = 1 \times 10^7$ cm s^{-1}.

The angular scattering associated with transitions for impact parameters $b < R_x$ for our test case can be crudely estimated assuming zero interaction in the initial channel and Coulomb scattering for the product channel. The Rutherford formula can be applied assuming half the trajectory follows the covalent and half the Coulomb potential, to obtain

$$\theta = \tfrac{1}{2}\pi - \cos^{-1}\left(\frac{\alpha}{(\alpha^2+4)^{1/2}}\right) \tag{13}$$

where

$$\alpha = \frac{2z_a z_b e^2}{\mu v_0{}^2 b} = \frac{z_a z_b e^2}{E_{cm} b} \tag{14}$$

and z_a and z_b are the charges of the product ions. For our case, $z_a = 5$ and $z_b = 1$, so that at $v = 1 \times 10^7$ cm s^{-1}

$$\alpha = \frac{2.8488}{b}. \tag{15}$$

Thus, a crude estimate of the minimum scattering angle will be to set $b = b_x = 8\, a_0$ and obtain $\theta = 8.8°$ at $v = 1 \times 10^7$ cm s^{-1}. Such an approach overestimates the minimum scattering angle because the particles do not follow an average potential for $b < b_x$. However, equations (13) and (14) do show the parameter dependence of the scattering angle which for small values of α is directly proportional to the product

of the final charge states and inversely proportional to collision energy and impact parameter.

One can use the procedure of Olson and Smith (1971) to obtain a more accurate estimate of the trajectories the particles follow for $b \leqslant b_x$. For $C^{6+}+H$ at $v = 1\times10^7$ cm s^{-1} ($E_{cm} = 47.8$ eV), the classical deflection functions are given in figure 3.

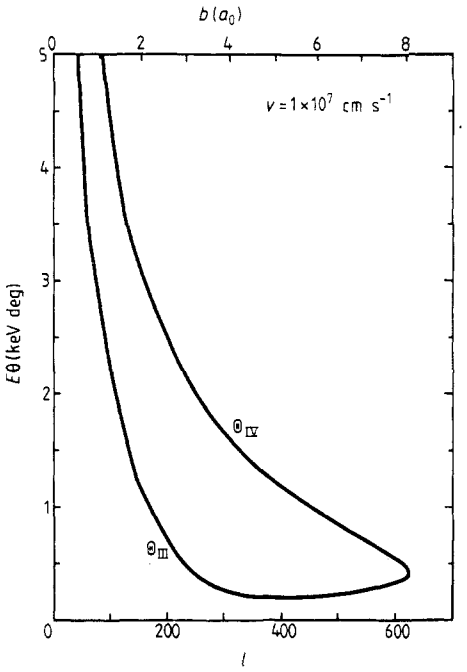

Figure 3. Classical deflection functions for the $C^{6+}+H$ reaction at $v = 1\times10^7$ cm s^{-1}. The notation is the same as used by Olson and Smith (1971).

For one branch, there is a large range of impact parameters, $4 \leqslant b \leqslant 7\ a_0$, for which the scattering is centred around $E\theta \simeq 0.2$ keV deg. These trajectories correspond to the particles following the diabatic covalent potential into the classical turning point and then switching to the repulsive Coulomb potential at R_x on the outward portion of the trajectory. Because two trajectories are possible for scattering to a given angle, Stueckelberg oscillations are expected with angular frequencies

$$\Delta\theta(\text{rad}) = \frac{2\pi}{l_{IV} - l_{III}} \tag{16}$$

where l_{III} and l_{IV} are the orbital angular momenta corresponding to scattering to angle θ.

The results of the differential scattering cross section calculations at $v = 1\times10^7, 2\times10^7$ and 3×10^7 cm s^{-1} ($E_{cm} = 47.8$, 191.0 and 429.8 eV, respectively) are presented in figure 4. Here, we have departed somewhat from the traditional 'rho–tau' plot and have used $\sin\theta\ d\sigma/d\Omega$ on the y axis because this is the quantity one integrates to obtain the total cross section

$$\sigma = 2\pi \int_0^{\pi} d\theta \sin\theta\ d\sigma/d\Omega. \tag{17}$$

Thus, it is easier to visualise the contribution of the large-angle scattering to the total cross section.

The differential cross sections displayed in figure 4 show an 'inelastic rainbow' at $\tau = E\theta \simeq 0.2$ keV deg due to the large range of impact parameters that contribute to the III branch of the deflection function, figure 3, and because $d\theta_{III}/dl = 0$. Stueckelberg oscillations follow at large angles. The integrated cross sections are within $\pm 25\%$ of the precise numerical values of Green *et al* (1981) and the benchmark measurements of Phaneuf (1981).

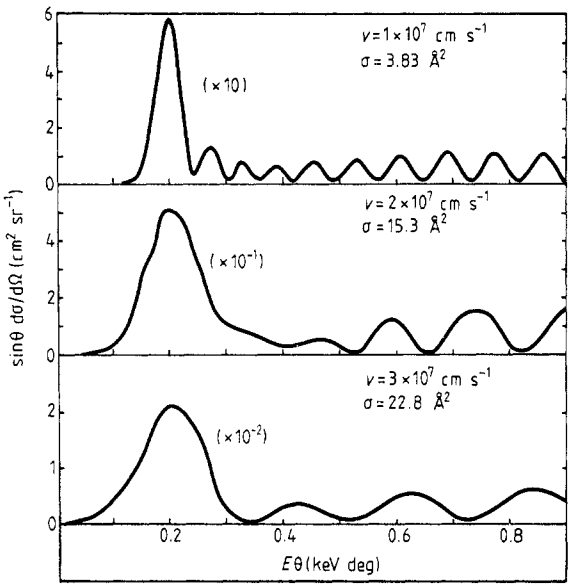

Figure 4. Reduced differential cross sections as a function of $\tau = E\theta$ for $C^{6+} + H \rightarrow C^{5+}(n = 4) + H^+$. Results for relative velocities of 1, 2 and 3×10^7 cm s^{-1} are presented.

The major reason for this work, however, is to emphasise the importance of large-angle scattering in reaction (1). Thus, displayed in figure 5 and presented numerically in table 1 are calculations giving the centre-of-mass angles required to observe fixed percentages of the electron capture total cross section. The large-angle scattering is appreciable and must be seriously considered in the design of an experimental apparatus to measure cross sections for reaction (1) at low velocities. If acceptance angles are not large enough, the measured cross sections will be too small.

The experimental acceptance angle requirement will not be as severe for the measurement of cross sections for heavy projectiles on light targets. For small angles and $E_{cm} \gg \Delta E$, laboratory scattering angles are related to the centre-of-mass angles by

$$\theta_{lab} \simeq \left(\frac{m_t}{m_t + m_p}\right)\theta_{cm} \tag{18}$$

where m_t and m_p are the masses of the target and projectile, respectively. Thus, for measurements on atomic or molecular hydrogen targets, few problems should arise. However, observation of low-velocity cross sections for light projectiles on heavy targets, such as $Ne^{q+} + Xe$, can lead to serious errors.

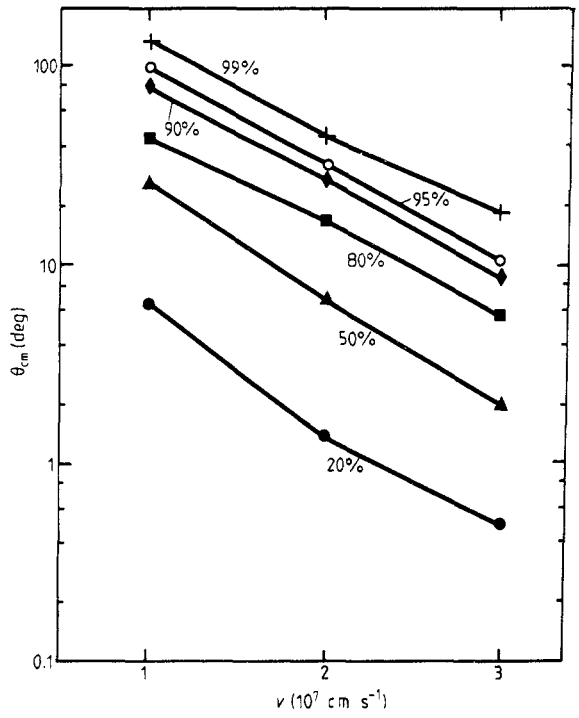

Figure 5. Centre-of-mass acceptance angles required to observe fixed percentages of the total electron capture cross section.

Table 1. Centre-of-mass acceptance angles required to observe fixed percentages of the total electron capture cross section for $C^{6+}+H$ collisions as a function of the relative collision velocity.

	v_{rel} (10^7 cm s^{-1})		
%	1.0	2.0	3.0
20	5.9°	1.4°	0.5°
50	26°	7.0°	2.1°
80	54°	17°	5.6°
90	78°	25°	8.5°
95	98°	29°	10°
99	150°	47°	19°
$\sigma_{6,5}$(10^{-16} cm^2)	3.83	15.3	22.8

4. Concluding remarks

The $C^{6+}+H$ system was used to illustrate the importance of large-angle scattering in electron capture reactions between multiply-charged ions and atoms at low collision velocities. The angular scattering is appreciable due to the deflection imparted by the Coulomb potential of the products. Thus, unless the angular deflection is recognised, experimental observations may underestimate the magnitude of the electron capture

cross sections, especially for light projectile ions on heavy target atoms or molecules. Likewise, final-state determinations in such measurements will preferentially sample only the large impact parameter collisions which populate the high-n principal quantum numbers of the $A^{(q-1)+}(n)+B^{+}$ products.

Acknowledgments

Research supported by the Magnetic Fusion Energy Division of the US Department of Energy.

References

Beyer H F, Schartner K H and Folkman F 1980 *J. Phys. B: At. Mol. Phys.* **13** 2459–73
Calogero F 1967 *Variable Phase Approach to Potential Scattering* (New York: Academic) Appendix I
Green T A, Shipsey E J and Browne J C 1981 *Phys. Rev.* A **23** 546–61
Johnson B R 1973 *J. Comput. Phys.* **13** 445–9
Justiniano E, Cocke C L, Gray T J, DuBois R D and Can C 1981 *Phys. Rev.* A **24** 2953–62
Makhdis Y Y, Birkinshaw K and Hasted J B 1976 *J. Phys. B: At. Mol. Phys.* **9** 111–21
Melius C F and Goddard W A III 1974 *Phys. Rev.* A **10** 1541–58
Messiah A 1958 *Quantum Mechanics* vol 1 (New York: Wiley) ch XI
Olson R E and Salop A 1976 *Phys. Rev.* A **14** 579–85
Olson R E and Smith F T 1971 *Phys. Rev.* A **3** 1607–17
Phaneuf R A 1981 *Phys. Rev.* A **24** 1138–41
Sharma S, Awad G L, Hasted J B and Mathur D 1979 *J. Phys. B: At. Mol. Phys.* **12** L163–6
Smith F T 1969 *Phys. Rev.* **179** 111–23
Thorson W R, Kimura M, Choi J H and Knudson S K 1981 *Phys. Rev.* A **24** 1768–79